The Cerebellum (2019) 18:406–421
https://doi.org/10.1007/s12311-019-1007-0

ORIGINAL PAPER

An Improved Method for Differentiating Mouse Embryonic Stem Cells into Cerebellar Purkinje Neurons

Christopher J. Alexander[1] · John A. Hammer[1]

Published online: 7 February 2019

Abstract

While mixed primary cerebellar cultures prepared from embryonic tissue have proven valuable for dissecting structure–function relationships in cerebellar Purkinje neurons (PNs), this technique is technically challenging and often yields few cells. Recently, mouse embryonic stem cells (mESCs) have been successfully differentiated into PNs, although the published methods are very challenging as well. The focus of this study was to simplify the differentiation of mESCs into PNs. Using a recently described neural differentiation media, we generate monolayers of neural progenitor cells from mESCs and differentiate them into PN precursors using specific extrinsic factors. These PN precursors are then differentiated into mature PNs by co-culturing them with granule neuron (GN) precursors also derived from neural progenitors using different extrinsic factors. The morphology of mESC-derived PNs is indistinguishable from PNs grown in primary culture in terms of gross morphology, spine length, and spine density. Furthermore, mESC-derived PNs express Calbindin D28K, IP3R1, IRBIT, PLCβ4, PSD93, and myosin IIB-B2, all of which are either PN-specific or highly expressed in PNs. Moreover, we show that mESC-derived PNs form synapses with GN-like cells as in primary culture, express proteins driven by the PN-specific promoter *Pcp2/L7*, and exhibit the defect in spine ER inheritance seen in PNs isolated from *dilute-lethal* (myosin Va-null) mice when expressing a *Pcp2/L7*-driven miRNA directed against myosin Va. Finally, we define a novel extracellular matrix formulation that reproducibly yields monolayer cultures conducive for high-resolution imaging. Our improved method for differentiating mESCs into PNs should facilitate the dissection of molecular mechanisms and disease phenotypes in PNs.

Keywords Mouse embryonic stem cells · Cerebellar Purkinje neurons · Cerebellar granule neurons · Co-culture

Introduction

The Purkinje neuron (PN) is the master neuron of the cerebellum. These large, highly dendritic cells receive most of the inputs into the cerebellum and are the sole output from the cerebellar cortex [1–3]. Either direct or indirect dysfunction of PNs leads to many degenerative neurological disorders. For example, spinocerebellar ataxias (SCAs) are a group of more than 40 heterogeneous, autosomal dominant, neurodegenerative diseases characterized by PN cell death, progressive ataxia, and cerebellar atrophy [4–8]. These diseases typically exhibit a progression from mild ataxia to eventual PN atrophy and severe ataxia (e.g., coordination of swallowing and breathing). There are currently no effective treatments or cures for SCAs.

Most studies addressing the etiology of SCAs have been performed using whole animals and fixed tissues (reviewed in [9]). While these studies have provided important insights into the molecular mechanisms underlying pathogenesis, additional insights would likely arise from studying SCA mutations in the context of mixed primary cerebellar cultures, as they have proven valuable for defining molecular mechanisms when combined with the PN-specific expression of genes using the PN-specific promoter *Pcp2/L7* [10–12]. Despite recent efforts to optimize this latter approach [12], it remains technically challenging and time-consuming and requires a sizeable number of animals, especially when studying mutant genes that must be maintained as heterozygotes.

Electronic supplementary material The online version of this article (https://doi.org/10.1007/s12311-019-1007-0) contains supplementary material, which is available to authorized users.

✉ John A. Hammer
hammerj@nhlbi.nih.gov

[1] Cell and Developmental Biology Center, National Heart, Lung, and Blood Institute, National Institutes of Health, Bethesda, MD, USA

An increasingly attractive alternative to using primary neuronal cultures is to create neuronal cultures from mouse embryonic stem cells (mESCs) [13–17]. mESCs are pluripotent stem cells with infinite proliferation properties and the potential to be differentiated into various cell/tissue types [18, 19]. Efforts to differentiate mESCs into neurons typically begin with the generation of neural progenitor cells from mESCs [20–23]. These neural progenitors are then differentiated into specific neuronal cell types using extrinsic factors that emulate the differentiation path the specific neuron follows during its development in vivo [24, 25]. The traditional approach to generating neural progenitors from mESCs involves the formation of large cell aggregates known as embryoid bodies, which form when mESCs are grown in the absence of an adhesive substrate and anti-differentiation factors like mouse leukemia inhibitory factor (mLIF) [26–29]. Embryoid bodies consist of a mixed population of cell types that "default" to the neuroectoderm lineage. As these neural progenitors produce extracellular matrix and begin to adhere to the culture dish, they form a characteristic radial arrangement of cell clusters known as rosettes. These rosettes are then specifically dissociated and cultured to generate an enriched population of neural progenitors for subsequent differentiation into specific neuronal cell types [30–32]. While this method has proven very effective at generating PN precursors, the formation of embryoid bodies and the subsequent selection of rosettes are both time-consuming and technically challenging. Moreover, as only the outermost cells of embryoid bodies are exposed to differentiation factors, and as interior cells undergo apoptosis, it is difficult to control the generation of neural progenitors from embryoid bodies [33].

Considerable effort has been made to define extrinsic factors that will promote the differentiation of mESCs into PNs. Early efforts showed that the addition of Fgf8b, Wnt proteins, BMPs, and retinoic acid to mESCs leads to the generation of cerebellar granule neurons (GNs) [34], the primary neuronal partner of PNs, and small numbers of Calbindin D28-positive PNs [35–37]. Subsequent efforts showed that the addition of just Fgf8 and Wnt1 to mESCs yields PNs, albeit still at a very low frequency (< 1%) [30, 37, 38]. Following this, pioneering work performed by Muguruma et al. showed that the differentiation of mESCs into PNs is made more efficient by the addition of the isthmic organizers insulin and fibroblast growth factor 2 (Fgf2), which are sufficient to activate a signaling pathway that augments the expression of Fgf8 and Wnt1 within the culture [31]. During development, PNs originate from the alar plate of rhombomere 1 [31, 39–41], and the addition of insulin and Fgf2 to embryoid bodies generates a subset of cells with a rhombomere 1 midbrain–hindbrain identity [31]. Muguruma and colleagues then went on to show that the addition of cyclopamine, a sonic hedgehog (Shh) inhibitor, in a time-restricted manner further promoted dorsalization and greatly improved the generation of PNs [31]. While this method has proven quite successful at generating PNs from mESCs, the cultures obtained are thick, making them hard to use for high-resolution light microscopy. Moreover, this method is labor intensive, as it requires the enrichment of PN precursor cells by FACS sorting, and their subsequent co-culture with GN feeder layers prepared separately from postnatal tissue.

Here we developed an improved method to differentiate mESCs into PNs that makes use of specific extrinsic factors and GN-like cells differentiated from mESCs rather than isolated from postnatal tissue. Our method circumvents the need to form embryoid bodies and subsequent rosette selection by employing a propriety differentiation medium (STEMdiff Neural Induction Medium, Stem Cell Technologies) that yields neural progenitor monolayers from mESCs in as few as 7 days. These neural progenitor monolayers are then used to separately generate PN precursors and GN precursors by the addition of specific sets of extrinsic factors. Finally, PN and GN precursors are mixed and plated on a novel extracellular matrix formulation to create monolayer cultures in which the PN precursors undergo final development over several weeks. We present multiple lines of evidence that these mESC-derived PNs are indistinguishable from PNs present in primary mixed cerebellar cultures. Our improved method for differentiating mESCs into PNs should prove valuable for the study of SCAs and other PN-related human diseases.

Methods

Primary Mixed Cerebellar Culture Cerebella from E17–E18 C57BL/6 (Charles River Laboratories) were harvested and cultured as described previously [12], except that cells were plated onto 14-mm aperture, 35-mm glass-bottom culture dishes (In Vitro Scientific, D35-14-1-N) coated with 0.01% (*w*/*v*) poly-l-lysine (Sigma, P8920) and grown in PN basal growth medium (DMEM/F12 containing 3.15 g/L (*w*/*v*) glucose, 3.57 g/L (*w*/*v*) HEPES (pH 8.0), 1 mM sodium pyruvate, 2.5 mM glutamine (Gibco, 11039), 1× N1 medium supplement (Sigma, N6530), 2 μM cytosine β-D-arabinofuranoside (ARA-C) (Sigma, C6645), 6 ng/mL tri-iodothyronine (T3) (Calbiochem, 64245), 25 ng/mL insulin-like growth factor I (IGFI) (Shenandoah Biotechnology, 100-34), 200 μg/mL transferrin (Sigma, T1147), 100 μg/mL bovine serum albumin (BSA) (Sigma, A3156), 20 μg/mL insulin (Sigma, I6634), and 5 μg/mL gentamycin (Gibco, 15710-064)). All cells were cultured at 37 °C, 95% humidity, and 5% CO_2.

Culture of mESCs Fibroblast feeder layer-free C57BL/6 embryonic stem cells from day 4 blastocysts were obtained from the NHLBI Transgenic Core (Dr. Chengyu Liu, NHLBI/NIH). To maintain pluripotency, cells were cultured on 2% gelatin (Sigma, G2500) in basal medium (IMDM with 4.5 g/L

glucose, 25 mM HEPES (pH 8.0), 4 mM L-glutamine (Gibco, 12440046), 15% ES-qualified FBS (ATCC, SCRR-30-2020), 1× nonessential amino acids (NEAA) (Gibco, 11140050), 0.2 mM 2-mercaptoethanol (β-ME) (Sigma, M6250)) supplemented with ESGRO-2i medium supplement (Millipore, ESG1124), which contains mLIF along with MEK1/2 and glycogen synthase kinase 3 (GSK3β) inhibitors to prevent spontaneous differentiation. Cells were cryopreserved at 1×10^6 cells per mL in STEM-CELLBANKER (Ambios, 11897F).

Induction of Neural Progenitors mESCs were washed with 1× PBS (pH 7.4) and dissociated from culture dishes using Accutase (Sigma, A6964) at 1 mL per 10 cm^2. Cells were counted using Cellometer Auto T4 cell counter (Nexcelom), and 2×10^5 cells in 500 μL were plated onto 14-mm aperture, 35-mm glass-bottom culture dishes coated with 1× Geltrex® (Thermo Fisher, A1569601). When cultures reached 80% confluency, the cells were washed with 1× PBS (pH 7.4), overlaid with proprietary Neural Induction Medium STEMdiff (Stem Cell Technologies, 05835), and cultured for 7 days, with a 75% medium change every other day to induce the formation of neural progenitors. Neural progenitor induction was confirmed by Western blots of whole cell extracts showing loss of expression of the stem cell marker Oct2 and expression of the neuroectoderm marker Pax6. Neural progenitors can be used immediately for differentiation into PNs and GNs or cryopreserved in 90% STEMdiff medium and 10% DMSO (Sigma, D2650).

Differentiation of Neural Progenitors into PN Precursors Neural progenitors were washed with 1× PBS (pH 7.4) and cultured in PN induction medium (DMEM/F12 containing 3.15 g/L (*w*/*v*) glucose, 3.57 g/L (*w*/*v*) HEPES (pH 8.0), 1 mM sodium pyruvate, 2.5 mM glutamine (Gibco, 11039) supplemented with 20 μg/mL transferrin (Sigma, T1147), 50 μg/mL BSA (Sigma, A3156), and 20 μg/mL insulin (Sigma, I6634)). Cells were cultured in this medium for 1 day, Fgf2 was added at a final concentration of 20 ng/mL, and the cells were cultured for an additional 9 days, with a medium change every other day. On day 7 through 10, cells were supplemented with cyclopamine (20 μM final concentration) to induce the formation of $Neph3^+$ PN precursors. PN precursors were dissociated from the culture vessel using Accutase and co-cultured with GN precursors (see below) to generate mature PNs. Note that we were not successful in differentiating PN precursors into mature PNs following cryopreservation and thawing.

Differentiation of Neural Progenitors into GN Precursors Neural progenitors were washed with 1× PBS (pH 7.4) and cultured in GN Induction Medium (DMEM/F12 with 3.15 g/L glucose and 1× GlutaMAX (Gibco, 10566016), and supplemented with 5% KnockOut serum replacement (Thermo Fisher, 10828028), 1× NEAAs, 0.1 mM β-ME, and 20 μg/mL insulin (Sigma, I6634)). After 2 days in culture, 50% of the media was exchanged with fresh media supplemented with 20 ng/mL epidermal growth factor (EGF), 0.5 mM bone morphogenic protein 4 (BMP4), 20 ng/mL Wnt3a, and 1 μM retinoic acid (RA), and the cells were cultured for an additional 5 days, with a 50% medium change every other day. Finally, the cells were cultured in media supplemented with Shh (100 ng/mL) and Jagged-1 (Jag1) (20 ng/mL) for 5 days to generate GN precursors. GN precursors can either be used directly for co-culture with PN precursors (see below) or cryopreserved in STEM-CELLBANKER for later use.

Co-culture of PN and GN Precursors PN precursors were mixed 1:1 with GN precursors at a final concentration of 2×10^6 cells/mL in PN basal growth medium supplemented with 1 μM of the activin receptor-like kinase receptor 5 (ALK5) inhibitor, SB 431542 (Caymen Chemical, 13031) [42]. Cells were plated on 14-mm aperture, 35-mm glass-bottom culture dishes (500 μL per dish) previously coated with 0.01% poly-l-lysine, 0.01% poly-l-ornithine and 1× Geltrex, and allowed to adhere for 2 h. Cells were then fed with 2 mL of fresh medium and incubated overnight. The following day, a 50% medium change was carried out and the cells were incubated for an additional 2 days. Following SB 431742 treatment, a complete medium change was carried out using complete PN growth medium. The following day, a 50% medium change was carried out and every 7 days thereafter.

Recovery of GN Precursors from Cryopreservation GN precursors frozen in liquid nitrogen were rapidly thawed in a 37 °C water bath with gentle agitation, transferred into 5 mL of fresh PN Basal Growth Medium, collected by centrifugation at 300×*g*, resuspended in 500 μL of PN basal growth medium, and plated onto a 14-mm aperture, 35-mm glass-bottom culture dish coated with 0.01% poly-l-lysine. Cells were allowed to adhere to the coverslip for 2 h before feeding with an additional 2 mL of medium. Upon reaching ~ 70% confluency, the cells were dissociated with Accutase and used for co-culture with PN precursors.

Immunofluorescence of Primary PNs and mESC-Derived PNs Cells cultured for 15–18 days were fixed for 30 min at room temperature in 4% paraformaldehyde (PFA) made by diluting a 16% PFA stock solution (Electron Microscope Sciences, 15710) using PBS (pH 7.4) (Gibco, 70011044) supplemented with 0.2% (*w*/*v*) picric acid (Sigma, 197378) [11]. Cells were washed three times with PBS, blocked for 30 min in IF blocking solution (10% (*v*/*v*) normal goat serum (EMD Millipore, S26-LITER), 1% (*w*/*v*) BSA, 0.5% (*v*/*v*) Triton X-100 (Sigma, T9824), and 2% (*w*/*v*) sucrose (Sigma, S7903) in

1× PBS (pH 7.4)). PNs were identified using anti-Calbindin D28K antibody (guinea pig, 1 to 500; Synaptic Systems, 214004). Depending on the experiment, cultures were also stained with the following primary antibodies at the indicated dilutions: anti-IP3R1 (mouse, 1 to 200; Santa Cruz, sc-271197), anti-AHCYL1 (IRBIT) (mouse, 1 to 200; Neobiolab, A7773), anti-PLCβ4 (mouse, 1 to 500; Santa Cruz sc-166131), anti-PSD93 (mouse, 1 to 200; Millipore, MABN497), or anti-myosin IIB-B2 (rabbit, 1 to 200; [43]) in 200 μL of IF blocking solution for 45 min at room temperature. Following three 10-min washes in PBS, samples were incubated at room temperature with 1 to 500 dilutions of the appropriate labeled secondary antibody (Alexa Fluor 546 goat anti-guinea pig, Thermo Fisher, A12074; Alexa Fluor 488 goat anti-mouse, Thermo Fisher, A11001; Alexa Fluor 488 goat anti-rabbit, Thermo Fisher, A11008). Samples were then washed three times with PBS (pH 7.4), overlaid with 200 μL of Fluoromount-G mounting medium (Electron Microscope Sciences, 179840-25), covered with 25 mm circular coverslip (Electron Microscope Sciences, 72223-01), and sealed with slide sealant. Images were obtained using a Zeiss LSM 780 laser scanning confocal microscope equipped with a Zeiss ×63, 1.4 NA oil objective.

Biolistic Expression of Exogenous DNAs Specifically in PNs Biolistic transfection of mESC-derived PNs with plasmid pKDMVa-2 [12], which drives the PN-specific expression of a miRNA directed against myosin Va, and plasmid pL7-mRFP-KDEL [11], which labels the PN's ER, was performed as described previously [44]. Briefly, gold particles were coated with DNA and introduced into GN and PN precursors 5 days after initiating co-culture using a Biolistic® PDS-1000/He Particle Delivery system (Bio-Rad, 1652257). Medium was removed from the culture just prior to bombardment. Immediately following bombardment, 50% of the saved (conditioned) medium was added to the culture along with 50% fresh basal growth medium. Cells were incubated for 2 days before a 50% medium changed was carried with fresh basal growth medium. From this point on, cells were cultured as normal with a 50% medium change every 7 days.

Western Blot Analyses At each point during differentiation, western blot analyses of specific markers were carried out. At each stage of differentiation, cells were dissociated from the culture dish and collected by centrifugation. Cells were lysed using RIPA buffer (50 mM Tris pH 7.4, 150 mM NaCl, 2 mM EDTA, 0.5% Na-deoxycholate, 1% NP-40, and 0.1% SDS supplemented with protease inhibitor cocktail). Total protein concentration was determined by a Bradford assay using BSA as a standard. Equal amounts of protein at each stage of differentiation were run on 4–20% SDS-PAGE gels and blotted on to PVDF using a semi-dry transblotter (Bio-Rad). Blots were probed for the following: stem cell marker anti-POU2F2 (Oct2) (rabbit, 1 to 1000; MyBioSource, MBS2526691), neural stem cell marker anti-Pax6 (rabbit, 1 to 1000; MyBioSource, MBS9205035), neuronal lineage marker anti-Tuj-1 (TubJ) (Rabbit, 1 to 1000; Santa Cruz, sc-58888), early GN marker anti-Math1 (rabbit, 1 to 1000; Santa Cruz, sc-98520), early PN marker anti-KIRREL2 (Neph3) (RABBIT, 1 to 1000; MyBioSource, MBS2519440), late GN marker anti-GABRA6 (rabbit, 1 to 1000; Santa Cruz, sc-7359), and late PN marker anti-Calbindin D28K antibody (rabbit, 1 to 1000; Osenses OSC00214W). Blots were washed extensively and incubated with the appropriate secondary antibody conjugated to HRP (anti-rabbit HRP, 1 to 10,000; GE Healthcare NA931-1ML; anti-mouse HRP, 1 to 10,000; GE Healthcare NA935-1ML). Bands were detected using a WesternBright ECL HRP detection system (Advansta, K-12045).

Image Analysis Stained cells were imaged using Zeiss LSM 780 confocal microscope equipped with 63x Plan Apo objectives (NA 1.4). All PN morphological analyses were carried out using Fiji [45]. To measure dendritic spine length, cells were fixed and stained with anti-Calbindin D28K, followed by Alexa 546-conjugated goat anti-guinea pig secondary antibody to mark cell volume. Serial 0.4-μm confocal sections that encompass the entire spine (identified using the cell volume marker Calbindin D28K in the 546-nm channel) together with the adjacent dendrite were summed using the Fiji Z projection function. Using the line tool, individual dendritic spines were masked by drawing a straight line from the tip of the spine head through to the dendrite at the base of the spine. Spine length was then determined by measuring the length of each corresponding line. To determine dendritic spine density, four serial 0.4-μm confocal sections (a total of 1.2 μm) were summed using the Fiji Z projection function. The length of the dendrite was then measured, and the number of dendritic spines was then manually counted. These data were used to determine the average number of dendritic spines per square micrometer. To determine the average cell footprint, cells were fixed and stained with anti-Calbindin D28K, and serial 1-μm confocal sections that encompass the entire cell were collected and summed using the Fiji Z projection function. Cells were then thresholded to mask the cell, the cell outline was determined using the automatic selection tool, and the total area within the selection was measured to determine the 2D cell footprint in square micrometers. All statistical analyses were performed using Student's *t* test.

Results

Simplified Method for Generating Neural Progenitors from mESCs Neural progenitors are traditionally obtained by growing embryoid bodies and then selecting rosettes [29–31]. Here

we used a proprietary neural differentiation media and other modifications to simplify the generation of mouse neural progenitors from mESCs. Briefly, mESCs that had been maintained in ESGRO-2i-supplemented medium prior to neural progenitor induction to ensure pluripotency (e.g., positive for the stem cell marker Oct2 [46, 47]; see Fig. 1 (yellow arrow) and Fig. 2, "mESCs") were dissociated from the dish using Accutase, washed in basal ESC medium without supplements, and cultured on Geltrex-coated dishes in basal ESC medium supplemented with insulin. At 80% confluency, the medium was changed to STEMdiff Neural Induction Medium to induce neural progenitor formation (Fig. 1, blue arrow). Neural progenitor generation was promoted by daily, 75% media replacements using fresh STEMdiff Neural Induction Medium for 5 days. Successful neural progenitor generation was confirmed by the expression of the neural progenitor marker Pax6 [48–57], the loss of expression of the mESC marker Oct2, and the expression of the neuron-specific tubulin isoform TubJ [58] (Fig. 2, "NPs"). While we typically used these monolayer neural progenitor cultures immediately to generate PN precursors (see below), we found that they can be saved for later use by harvesting them using Accutase and gentile agitation, and then cryopreserving them in liquid nitrogen using in 90% (*v*/*v*) STEMdiff Neural Induction Medium and 10% (*v*/*v*) DMSO (Fig. 1, blue snowflake). In summary, our improved method for generating neural progenitors from mESCs eliminates the need for embryoid body formation and rosette selection, yields monolayers of neural progenitors, and can be done in about half the time as traditional embryoid body-based methods.

Improved Method for Generating PN Precursors from Neural Progenitors As discussed in the "Introduction," the work of Muguruma et al. [31] and others [32] has shown that the addition of Fgf2 and insulin, together with the inhibition of Shh signaling, is sufficient to generate PN precursors from neural progenitors [31, 32]. We used a modification of this approach to generate PN precursors (Fig. 1, green arrow). Specifically, neural progenitor monolayers were grown to 80% confluency in STEMdiff Neural Induction Medium and then switched to PN induction medium containing insulin and transferrin. After 1 day, Fgf2 was added to the media and the cells were cultured for an additional 9 days, with medium changes every other day. Additionally, Shh signaling was inhibited from day 7 through day 10 by the addition of cyclopamine to the medium. Previous studies have shown that

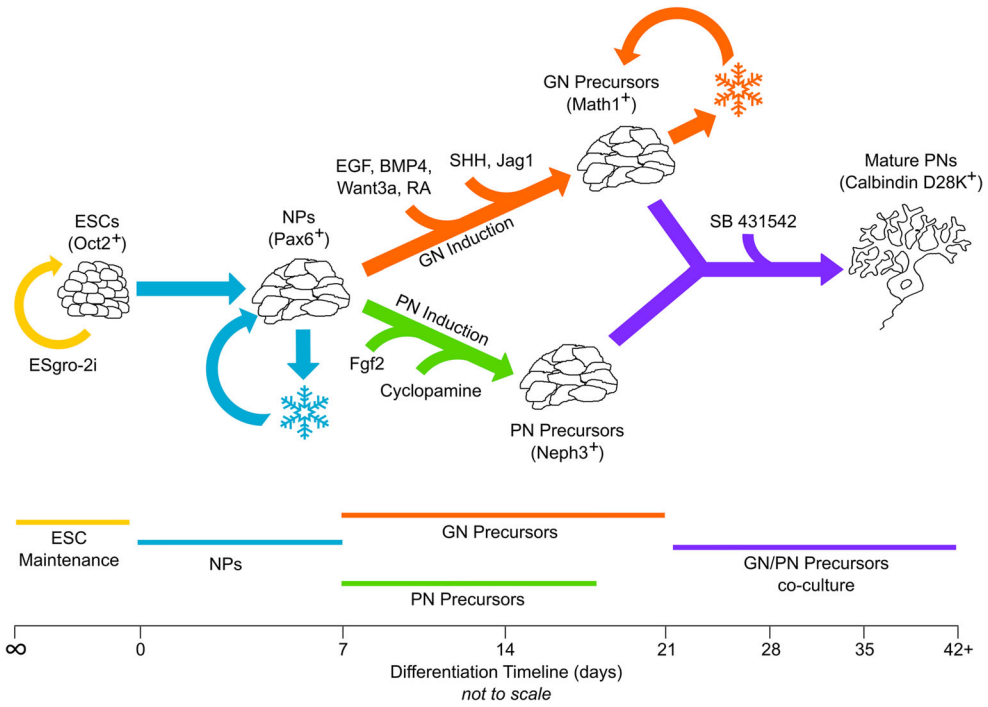

Fig. 1 Flow diagram for the generation of Purkinje neurons from mESCs. Pluripotent, Oct2-positive mESCs are maintained in ESGRO-2i containing medium (yellow arrow). mESCs are differentiated into Pax6-positive neural progenitors (NPs) using STEMdiff Neural Induction Medium, as described in the text (blue arrow). NPs can be cryopreserved for later use (blue snowflake). Using two distinct sets of extrinsic morphogens and growth factors (see figure and text), NPs are then differentiated separately into Math1-positive granule neuron (GN) precursors (orange arrow) and Neph3-positive Purkinje neuron (PN) precursors (green arrow). GN precursors can be cryopreserved for later use (orange snowflake). Finally, GN precursors and PN precursors are co-cultured in the presence of the TGFßR1 antagonist SB 431542 (see figure and text) to generate fully developed PNs that, by several criteria, are indistinguishable from mature PNs present in primary mixed cerebellar cultures. A timeline is shown at the bottom of the diagram that starts with the induction of NPs (day 0) and progresses through the generation of PNs (day 42 onwards). Note that the timeline is not drawn to scale

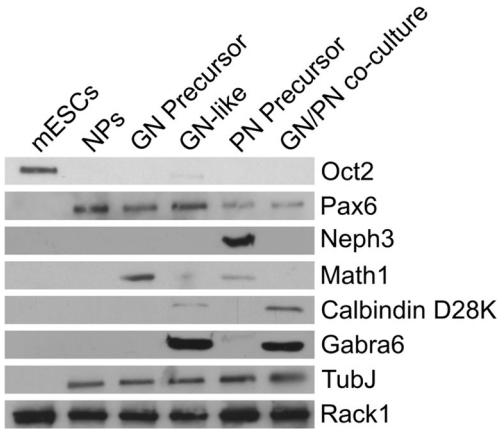

Fig. 2 Diagnostic Western blots to follow the differentiation of mESCs into PNs. Shown are Western blots performed on whole cell extracts from the cells indicated at the top using antibodies to the markers shown on the right. mESCs are positive for the pluripotency marker Oct2, NPs are positive for the early neural marker Pax6, GN precursors are positive for the early GN marker Math1, GN-like cells obtained by extended culture of GN precursors (see text) are positive for the GN-specific GABA receptor subunit GABRA6, PN precursors are positive for the early PN marker Neph3, GN-like cells present in day-21 GN/PN precursor co-cultures are positive for GN-specific GABA receptor subunit GABRA6, and mature PNs in day-21 GN/PN precursor co-cultures are positive for the PN-specific marker Calbindin D28K. All neuronal lineages are positive for the neuron-specific tubulin isoform TubJ. Probing for the ubiquitously expressed scaffolding protein RACK1 was used to show equal protein loads

by this point most Neph3-positive cells in cultures are PN precursors [30–32]. Consistently, the expression of this early PN marker was evident in Western blots of day-10 whole cell extracts (Fig. 2, "PN precursors"). Moreover, staining of day-10 cultures for Neph3 and TubJ indicated that ~10% of the cells in these cultures are PN precursors (Fig. S1). At this point, other protocols use FACs sorting to enrich the population of Neph3-positive cells, which are then co-cultured with GN feeder layers prepared separately from postnatal cerebellar tissue. Here we sought to promote the differentiation of PN precursors into PNs by mixing day-15 cultures directly with GN precursors that were differentiated in parallel from neural progenitors, as described next.

Generation of GN Precursors from Neural Progenitors As highlighted in the "Introduction," GNs are required for PNs to develop in culture and remain healthy [36]. Careful examination of the literature [35, 37, 59–60] revealed that the generation of GN precursors from neural progenitors is fairly similar to the generation of PN precursors from neural progenitors, with the major difference being that Shh signaling, which inhibits PN differentiation, is required for GN differentiation. Based on this and other information [35, 37], we developed a simplified method to generate GN precursors from neural progenitors (Fig. 1, orange arrow) that could be performed in parallel with the generation of PN precursors from neural progenitors described above and that would dovetail with the latter for final co-culture. Specifically, neural progenitor monolayers were grown to 80% confluency in STEMdiff Neural Induction Medium and then switched to GN induction medium supplemented with insulin. After 2 days, EGF, BMP4, Wnt3a, and retinoic acid were added to the media and the cells cultured for an additional 5 days, with 50% media changes performed every other day. On day 7, the cells were switched to GN induction medium supplemented with Shh and Jag1 and cultured for an additional 5 days, with 50% media changes performed every other day. Importantly, Western blots of whole cell extracts prepared from day-12 cultures revealed the expression of Math1 (also known as Atoh1), a transcription factor required for GN differentiation (Fig. 2, "GN precursors") [34, 41, 61–65] (note, however, that Math1 is not GN-specific). Moreover, day-12 cultures contained large numbers of cells exhibiting a typical GN morphology and expressing NeuN, a marker expressed by cerebellar GNs [66–69] (Fig. S1) (note, however, that NeuN is not GN-specific). Finally, day-12 cultures were grown for an additional 3 to 5 days in complete PN growth medium, at which time they were either mixed with PN precursor cultures to drive complete PN differentiation as described below or cryopreserved for later use (Fig. 1, orange snowflake). We note that while the differentiation of PN precursors described in the previous section appears to yield some cells that are positive for the GN differentiation marker Math1 (Fig. 2, see the faint Math1 band in "PN precursors"), these Math1-positive cells must not be present in enough numbers to support the differentiation of PN precursors in mature PNs. We also note that if one continues to culture GN precursors for 14 days in PN basal growth medium, they will form a culture enriched in neurons positive for the late GN marker GABRA6 [70–73] (Fig. 2, "GN-like"). While these cultures do appear to contain some cells that are positive for the mature PN marker Calbindin D28K (Fig. 2, see the faint Calbindin D28K band in "GN-like"), these Calbindin D28K-positive cells do not develop dendritic arbors characteristic of PNs in primary culture (Fig. S2).

Co-culture of PN Precursors and GN Precursors The traditional approach for differentiating mESC-derived neurons is to layer them on top of an embryonic feeder layer that serves to support the growth and development of the neurons [15, 37]. Attempts to layer PN precursors on top of cultures of GN precursors resulted in poor PN precursor attachment and a very low yield of developed, Calbindin D28K-positive PNs. Given this, we decided to mix PN and GN precursor cultures together before plating, reasoning that this starting environment would mimic the starting material used in traditional mixed primary cerebellar cultures. To accomplish this, the mixed-cell populations present in both precursor PN and precursor GN cultures were carefully dissociated by gentle

Accutase treatment, washed once in complete PN growth medium, mixed 1:1, and allowed to attach to glass-bottomed dishes (Fig. 1, purple arrow). Because immature PNs express Skor2/Corl2, a c-Ski transcription factor that acts as a TFG beta 1 receptor (TGFßR1) antagonist, and that is important for PN development [37–39, 74, 75], cultures were supplemented with the TGFßR1 antagonist SB 431542 for 2 days to improve PN differentiation (this addition improved the number of developed PNs by approximately 25%, generating a similar number of cells as primary cultures; see below). Following treatment with SB 431542, cultures were subjected to a complete medium change using complete PN growth medium (the same medium used to grow PNs in mixed primary cerebellar cultures). A 50% medium change was carried out the following day, followed by 50% medium changes every 7 days thereafter. Western blots of this culture showed strong signals for both the mature PN marker Calbindin D28K [10, 12, 76–80, 81] and the mature GN marker GABRA6 [72, 82, 83] (Fig. 2, see "GN/PN co-culture"). Finally, we found that gelatin is not a suitable substrate for co-culturing these cells because it results in large cell aggregates (Fig. S3A). By contrast, plating on a mixture of Geltrex, poly-l-lysine (PLL) and poly-l-ornithine (PLO) (see "Methods") yielded highly reproducible mixed monolayer cultures conducive for high-resolution microscopy (Fig. S3B).

Finally, we note that variations in many factors (e.g., reagents, serum) affect the differentiation and growth of mESC-derived PNs just as they do for primary PNs. For this reason, it is not feasible to determine the precise efficiencies of the various steps in our method. That said, our final mESC-derived PN cultures reproducibly contain a similar number of PNs as seen in primary PN cultures (Fig. S4).

PNs Derived from the Co-culture of PN and GN Precursors Appear Indistinguishable from PNs Present in Mixed Primary Cerebellar Cultures We used immunofluorescence staining with an antibody to Calbindin D28K, a well-established PN-specific marker [10, 76, 77, 84–87], to follow the development of PNs in co-cultures of PN precursors and GN precursors. Calbindin D28K-positive cells were readily apparent in these co-cultures 7 days post-SB 431542 treatment (Fig. 3A1), at which point they exhibited immature dendritic arbors typical of immature PNs present in mixed primary cerebellar cultures after 7 days in vitro (Fig. 3B1). Importantly, by 21 days post-SB 431542 treatment, the Calbindin D28K-positive cells in PN/GN precursor co-cultures (Fig. 3A2) exhibited a gross morphology typical of mature PNs present in primary cerebellar cultures after 21 days in vitro (Fig. 3B2) (note, however, that mESC-derived PNs, like PNs in primary culture, are not as highly arborized as PNs in situ; see "Discussion"). Moreover, like mature PNs in primary culture, the dendritic spines of Calbindin D28K-positive cells in PN/GN precursor co-cultures 21 days post-SB 431542 treatment were covered with dendritic spines (compare Fig. 3A3 to Fig. 3B3). Importantly, the Calbindin D28K-positive cells in mESC-derived PN cultures exhibited average spine lengths and spine densities at 21 days post-SB 431542 treatment that were not significantly different from mature PNs present in primary cerebellar cultures after 21 days in vitro (Fig. 3C, D, respectively; $n = 15$ cells each; $p = 0.36$). Moreover, mESC-derived PNs are not significantly different from mature primary PNs with regard to the number of primary dendrites (mESC-derived PNs, 2.19 ± 0.98 ($n = 15$ cells); primary PNs, 1.86 ± 0.89 ($n = 15$ cells), ($p = 0.35$)), the number of primary dendritic branch points (mESC-derived PNs, 2.63 ± 0.89 ($n = 32$ dendrites across 15 cells); primary PNs, 2.53 ± 1.06 ($n = 28$ dendrites across 15 cells) ($p = 0.27$)), or the overall cellular footprint (mESC-derived PNs, 475 ± 183 μm^2 ($n = 8$ cells); primary PNs, 512 ± 78 μm^2 ($n = 8$ cells) ($p = 0.52$)). Together, these results argue that the co-culture of PN precursors and GN precursors derived from mESCs gives rise to bona fide PNs.

To provide further support for our conclusion that mESC-derived, Calbindin D28K-positive cells are bona fide PNs, we co-stained them for five proteins that are known to be expressed by PNs (Fig. 4). As with mature PNs in tissue [78–80] and in primary culture (Fig. S5), the dendritic spines of mESC-derived PNs stain robustly for the PN-specific post-synaptic density protein PSD93 [10, 78, 87, 88] (Fig. 4A1–A4) and for the PN-specific isoform of phospholipase C, PLCβ4 [79] (Fig. 4B1–B4). Also, like PNs in tissue and primary culture (Fig. S5), mESC-derived PNs stain robustly at the base of their spines for a PN-specific splice isoform of nonmuscle myosin IIB (nonmuscle myosin IIB-B2; [43, 89]) (Fig. 4C1–C4). Finally, like PNs in tissue [90–92] and primary culture [10–12] (Fig. S5), essentially every spine in mESC-derived PNs contains smooth endoplasmic reticulum (SER), as evidenced by staining for IP3 receptor 1 (IP3R1) (Fig. 4D1–D4) and for the IP3R1-associated protein IRBIT [93] (Fig. 4E1–E4). Of note, the presence of SER in virtually every spine is a unique property of PNs [10, 94, 95].

To ascertain whether the co-culture of PN precursors and GN precursors also leads to the generation of GNs, we stained co-cultures at 28 days post-SB 431542 treatment with anti-Calbindin D28K to mark PNs and either an antibody to tubulin J to mark all neurons (Fig. 5A1–A3), or an antibody to the alpha6 subunit of gamma-aminobutyric acid type A receptor (GABRA6), which is often used as a GN marker [96–98] (Fig. 5B1–B3). Co-staining for Calbindin D28K and tubulin J shows that these PN/GN precursor co-cultures contain neurons other than PNs, many of which exhibit the morphology of GNs (see arrowheads in Fig. 5A2–A3). Moreover, co-staining for Calbindin D28K and GABRA6 shows that many of these additional, Calbindin D28K-negative neurons exhibit a punctate staining for GABRA6 that is typical of GNs [97] (see arrowheads in Fig. 5B2–B3; also see the arrows, which

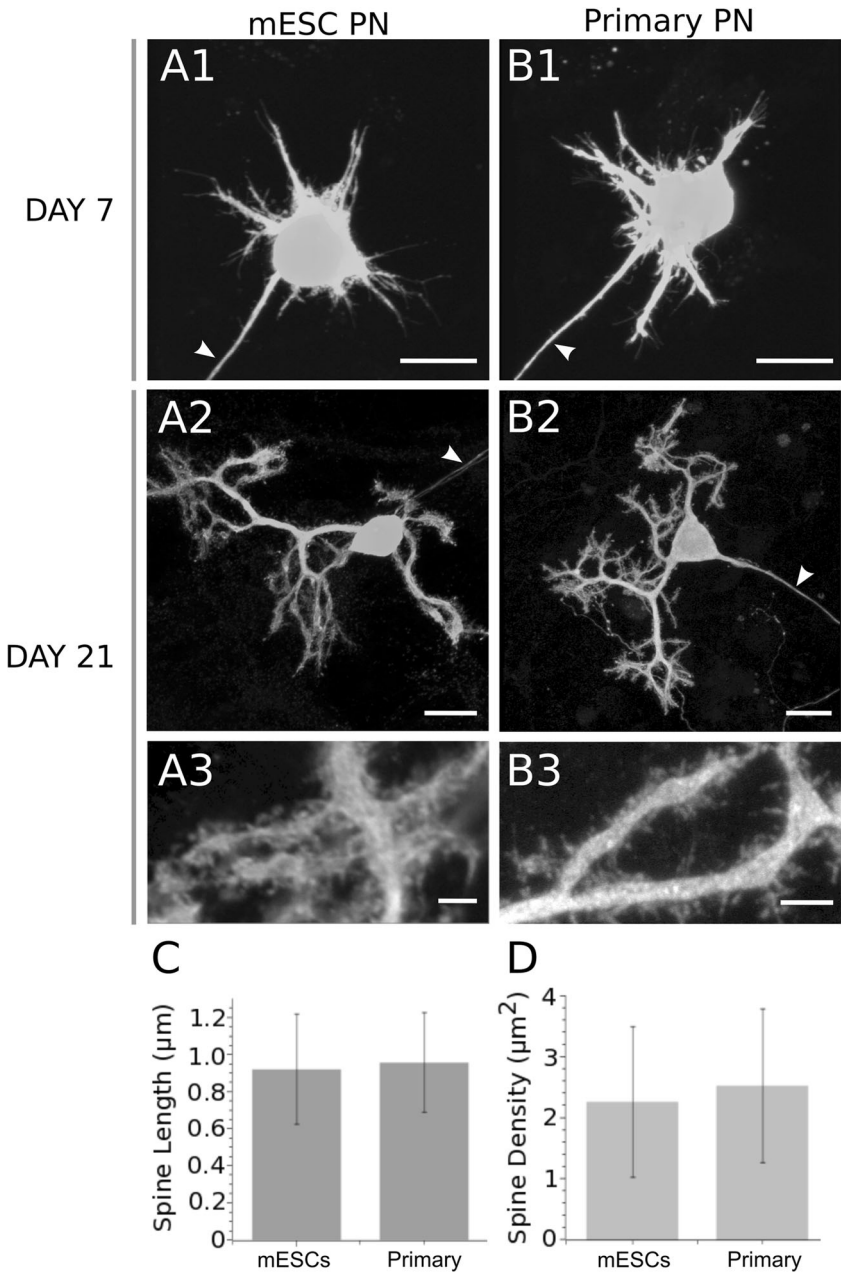

Fig. 3 mESC-derived PNs are indistinguishable morphologically from primary PNs. Shown are Calbindin D28K-stained, mESC-derived PNs present within a GN/PN co-culture 7 and 21 days post-SB 431542 treatment (A1 and A2, respectively), and Calbindin D28K-stained primary PNs after 7 and 21 days in vitro (B1 and B2, respectively). The boxed regions in A2 and B2 are shown at higher magnification in A3 and B3, respectively. The average lengths (in μm) and densities (in number/μm^2) of dendritic spines in day-21 mESC-derived PNs and day-21 primary PNs are shown in C and D, respectively. A total of 15 cells from three independent preparations of mESC-derived and primary cultures were analyzed to determine spine length and spine density ($n = 111$ (mESC) and 104 (primary)). Both values for mESC-derived PNs are not significantly different from the values for primary PNs. Mag bars = 20 μm (A1 and B1), 20 μm (A2 and B2), and 5 μm (A3 and B3). Cells were selected by scoring the first PN viewed upon focusing the microscope on the GN/PN co-culture, and then scoring the nearest four PNs (only PNs that were clearly dying were excluded). Arrowheads mark the axon (based on morphology) belonging to the mESC-derived PN (A1–A2) and the primary PN (B1–B2)

point to one such neuron immediately adjacent to a PN dendrite). While these observations, together with the fact these cells are clearly supporting PN differentiation like bona fide GNs do, argue that our mESC-derived cultures also yield bona fide GNs, in the absence of additional GN markers, we refer to them as GN-like (see "Discussion").

We next sought to provide evidence that PNs derived from mESCs form synapses with these GN-like cells, just as PNs in primary mixed cerebellar cultures form synapses with bona fide GNs [96, 98–100]. To accomplish this, we stained mESC-derived cultures and primary mixed cultures for Calbindin D28K to mark PN spines and for Bassoon, which marks presynaptic active zones in GNs [101, 102] (note, however, that Bassoon is not GN-specific). Figure 6 shows that the Bassoon signal appears as dots immediately adjacent to PN spines in mESC-derived cultures (Fig. 6A1–A4), as well as in primary mixed cultures (Fig. 6B1–B4). Images of individual spines (Fig. 6A5, B5) and accompanying line scans (Fig. 6A6, B6) show that Bassoon-positive presynaptic active zones indeed lie immediately adjacent to spines for both mESC-derived PNs and primary PNs. We conclude, therefore, that mESC-derived PNs form synapses with GN-like cells just like PNs in primary mixed cerebellar cultures form synapses with bona fide GNs.

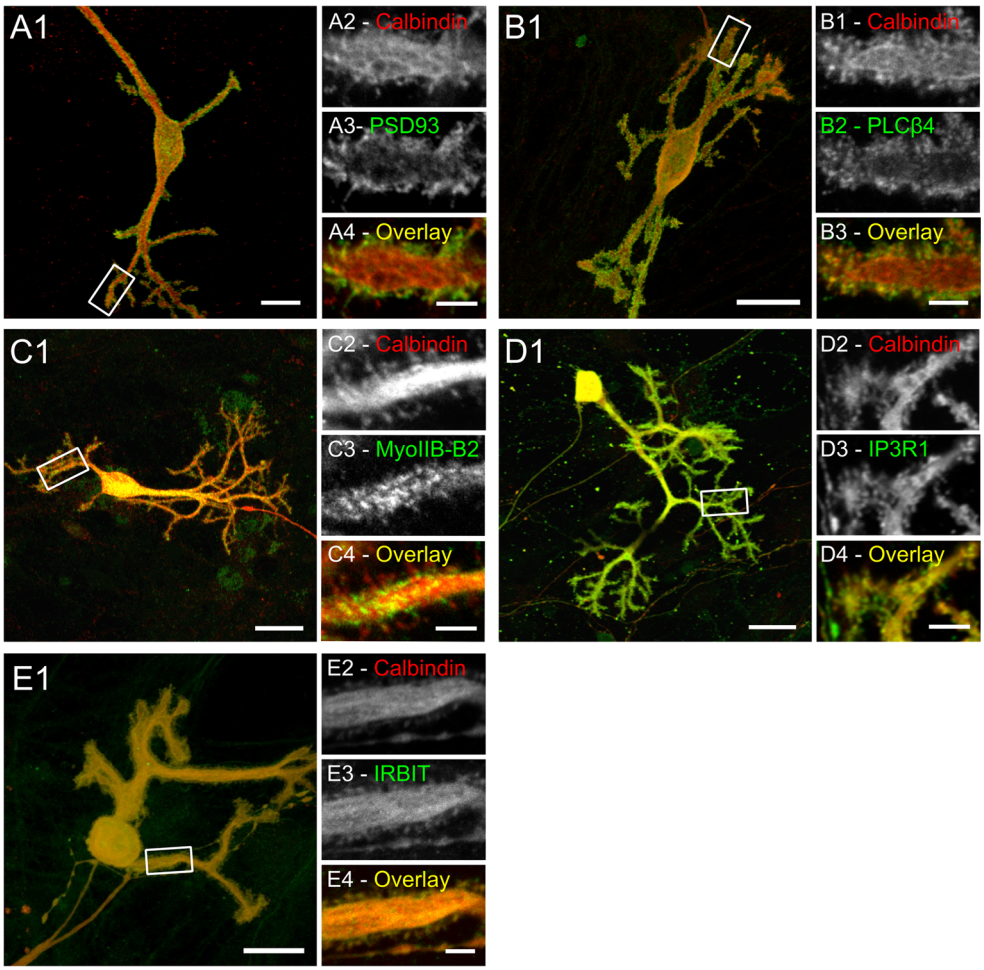

Fig. 4 mESC-derived PNs express multiple proteins used previously to mark PNs. Shown are representative examples of day-21 mESC-derived PNs present within a GN/PN co-culture that were double-stained for the PN-specific protein Calbindin D28K in red and the following proteins known to be expressed by PNs in green: PSD93 (A1–A4), PLCβ4 (B1–B4), myosin IIB-B2 (C1–C4), IP3R1 (D1–D4), and IRBIT (E1–E4). Each sample is presented as a lower magnification, overlaid image in the first panel, and higher magnification split and overlaid images of the boxed region in the second, third, and fourth panels, respectively. Mag bars = 20 μm (A1–E1) and 5 μm (A4–E4)

Previous efforts by us [9–11] and others [94, 103–105] have shown that genes can be expressed specifically within PNs present in mixed primary cerebellar cultures using the PN-specific promoter *Pcp/L7*. Consistent with our conclusion that our mixed mESC-derived cultures contain bona fide PNs, introduction of a custom plasmid [11] driving the expression of free GFP downstream of the *Pcp/L7* promoter into these cultures (Fig. S6A1 and the inset in S6A2) results in green neurons exhibiting a morphology that is indistinguishable from similarly treated PNs present in primary mixed cultures (Fig. S6B1 and inset in S6B2).

As mentioned above, PNs are unique among CNS neurons in having essentially every spine filled with SER [10, 94, 106]. In striking contrast, the spines of PNs present in mice that lack myosin Va (*dilute* mice) are essentially devoid of SER [10, 94]. The functional consequence of this dramatic defect is the complete loss of synaptic plasticity at the GN–PN synapse and, at the animal level, severe ataxia [107, 108]. This and other data [10] have established that myosin Va serves to transport SER in PN spines. As a final test of mESC-derived PNs, we asked if the knockdown of myosin Va in them results in the loss of SER from their spines. Consistent with previous studies of wild-type PNs in primary culture [10, 12], untreated WT mESC-derived PNs expressing free GFP to mark cell volume and RFP-KDEL to mark the SER exhibit tubules of SER in essentially every spine (Fig. 7A1–4, D). Moreover, like *dilute* PNs in primary culture [10], WT primary PNs expressing free GFP, RFP-KDEL, and a validated miRNA directed against myosin Va exhibit spines that are essentially devoid of SER (Fig. 7B1–B4; see also [12]). Finally, WT mESC-derived PNs expressing free GFP, RFP-KDEL, and this myosin Va-specific miRNA also exhibit spines that are essentially devoid of SER (Fig. 7C1–C4, D). Taken together, the data presented above provides very strong evidence that our mESC-derived cultures contain bona fide PNs.

Discussion

In this study, we presented an improved method for differentiating mESCs into cerebellar PNs. Our method begins with a simplified protocol for generating neural progenitors from mESCs that eliminates the need for embryoid body formation and rosette selection, yields monolayers of neural progenitors,

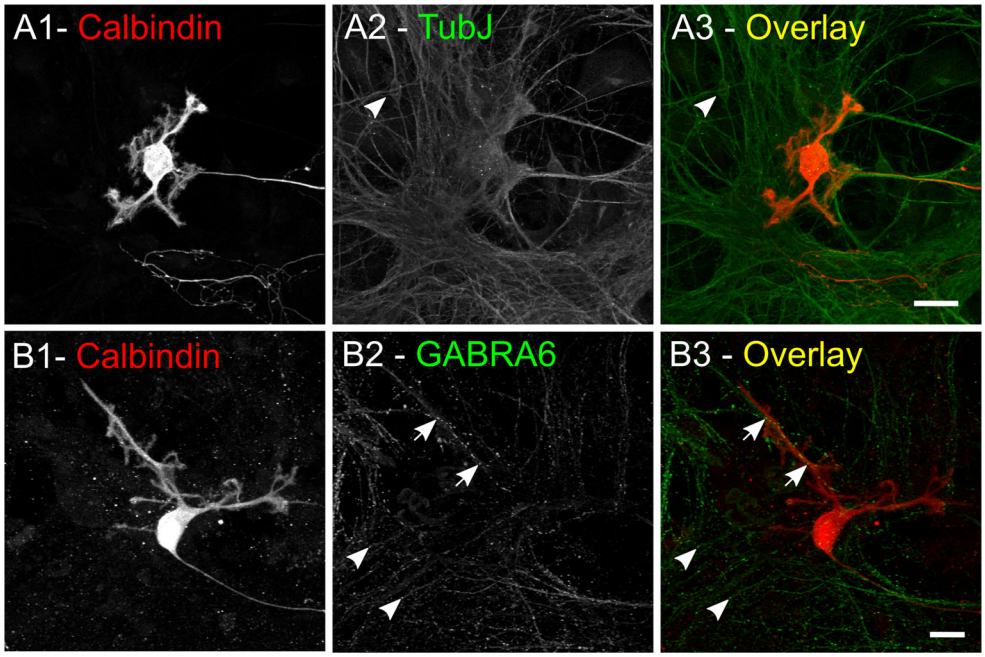

Fig. 5 GN-like cells are present in mESC-derived PN cultures. Shown is a representative example of a day-21 mESC-derived PN present within a GN/PN co-culture that was double-stained for the PN-specific marker Calbindin D28K in red (A1) and the neuronal marker TubJ in green (A2). The corresponding overlaid image is shown in A3. The arrowheads in A2 and A3 point to a TubJ-positive neuron that is not a PN. Also shown is a representative example of a day-21 mESC-derived PN culture that was double-stained for the PN-specific marker Calbindin D28K in red (B1) and the GN-specific marker GABRA6 in green (B2). The corresponding overlaid image is shown in B3. The arrowheads in B2 and B3 point to a Calbindin D28K-negative neuron that is positive for the GN-specific marker GABRA6. The arrows point to a similar neuron that is immediately adjacent to the dendrite of a Calbindin D28K-positive PN. We note that only a small fraction of the PN precursors added at time 0 develop into PNs, resulting over time in an excess of GN-like cells. We also note that altering the starting ratio of GN precursors to PN precursors could further improve the yield of mature PNs. That said, the starting ratio we used (1:1) gives a density of PNs in the final culture that is similar to what we see in the primary culture. Moreover, this density is ideal for high-resolution imaging of PNs and more than sufficient for detailed structure–function analyses. Mag bars = 20 μm (A3) and 5 μm (B3)

and can be done in about half the time as traditional embryoid body-based methods. Using a distinct set of extrinsic morphogens and growth factors that mirror in vivo cerebellar development, we then separately differentiate these neural progenitors into PN precursors and GN precursors. Finally, these PN and GN precursors are co-cultured, leading to the differentiation of the PN precursors into PNs that appear indistinguishable from mature PNs present in primary cerebellar cultures. By avoiding the use of postnatal feeder layers that are associated with other protocols for differentiating mESCs into PNs, our improved method also saves on animal costs.

We presented multiple lines of evidence that our method yields bona fide PNs from mESCs. First, the cells have an overall morphology that is indistinguishable from PNs present in traditional, mixed primary cerebellar cultures (Fig. 3 and text). Second, the cells stain for six markers used previously by us and others to identify PNs, with each localizing to its correct cellular compartment (Figs. 3, 4, and S5). While there may be no marker that is absolutely PN specific, our use of six markers that are specific to PNs in mixed primary cerebellar cultures (Fig. S5 and [43, 78–80, 89–92]) exceeds what is commonly provided as evidence for the creation of bona fide PNs from stem cells (see for example Watson et al. [65], where only two markers were used to argue that bona fide PNs had been generated from IPSCs). Third, the cells express proteins under the control of the PN-specific promoter *Pcp2/L7* (Fig. S6). Finally, the expression of a myosin Va-specific miRNA in the cells leads to the loss of spine SER targeting, just as seen in PNs isolated from *dilute*/myosin Va-null mice (Fig. 7) [10, 94, 95].

We referred to other cells in our final mESC-derived cultures as GN-like rather than GNs because we have not shown categorically that they are bona fide GNs. That said, our GN precursor cultures express the transcription factor Math1 (Fig. 2), which, while not GN-specific, is required for GN differentiation [34, 41, 60–65]. Moreover, cells in our final co-cultures that exhibit the morphology of GNs stain with an antibody to the alpha6 subunit of GABRA6, which is often used as a GN marker [96–98] (Fig. 5). These cells also form Bassoon-positive synapses with the PNs in the co-culture (Bassoon marks GN–PN synapses in both

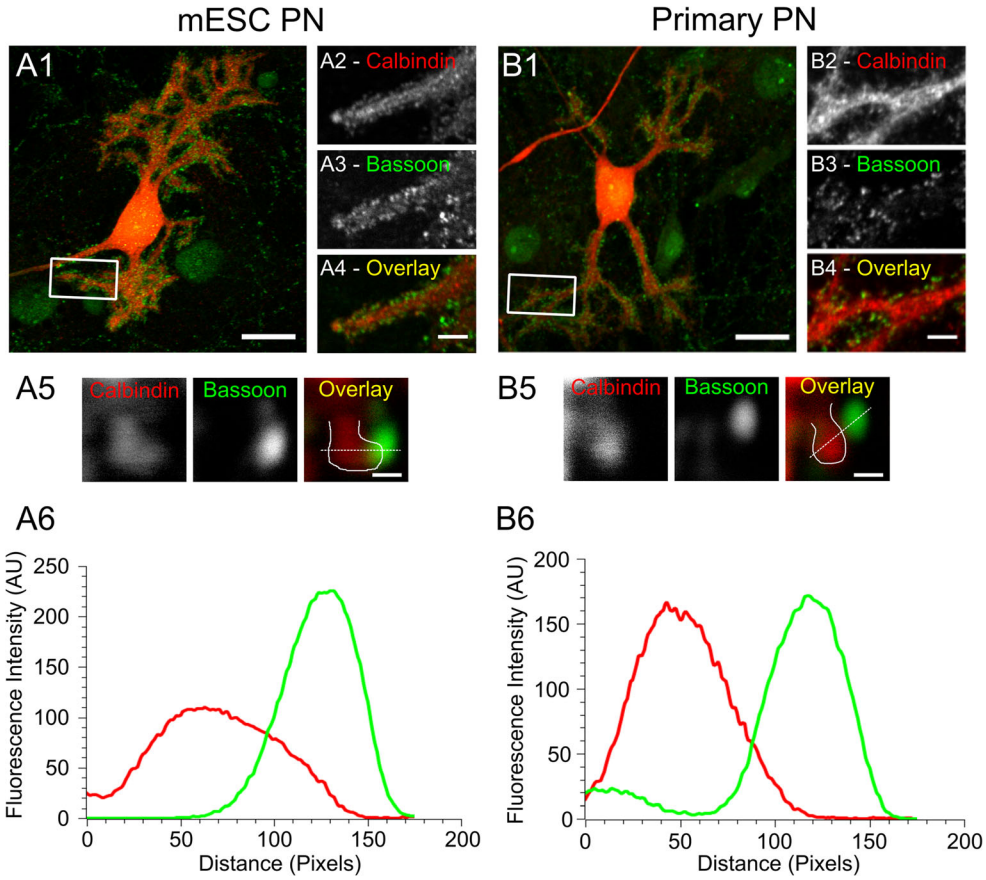

Fig. 6 mESC-derived PNs form synapses with GN-like cells in the culture. Shown are representative examples of a day-21 mESC-derived PN present within a GN/PN co-culture (A1–A4) and a day-21 PN present in a primary culture (B1–B4) that were double-stained for the PN-specific marker Calbindin D28K in red and the presynaptic active zone marker Bassoon in green. A1/B1 show a lower magnification, overlaid image, while A2/B2, A3/B3, and A4/B4 show higher magnification split and overlaid images of the boxed regions in A1 and B1. A5 and B5 show high magnification split and overlaid images for Calbindin D28K (red) and Bassoon (green) at a single, representative spine on a mESC-derived PN and a primary PN, respectively. In both cases, the PN spine head is outlined with a solid white line, and the orientation of the line scan that was performed across the synapse is shown by the dotted line. A6 and B6 show the signals for Calbindin D28K in red and Bassoon in green for the spine line scans marked in A5 and B5, respectively. Mag bars = 20 μm (A1 and B1), 5 μm (A4 and B4), and 0.5 μm (A5 and B5)

primary mixed cerebellar cultures and tissues; [97, 99, 100, 103]) (Fig. 6). Finally, given that GNs are known to be critical for the growth and development of PNs, the presence of developed PNs in our final culture argues that these GN-like cells are indeed GNs. Assuming this is the case, specific manipulation of these cells using a GN-specific promoter [109] should prove valuable, especially as GNs are the primary source of synaptic input for PNs.

We note two other ambiguities in our method besides the remaining question regarding the exact identity of the GN-like cells. First, our mESC-derived cultures may lack some cell types that are present in primary PN cultures and/or in tissue. Given that these cells might make significant contributions to PN function, future efforts should be directed at identifying all the cell types present in our mESC-derived cultures, and possibly supplementing these cultures with additional cell types. Second, while we refer to the PNs present in our final co-culture as mature because they are indistinguishable from PNs present in mixed primary cerebellar cultures, neither exhibit dendritic arbors that are as extensive as PNs in situ. While this observation suggests that the culturing of PNs may not completely recapitulate the differentiation and development of PNs in vivo, what is clear is that our mESC-derived PNs, like primary PNs [10], can be used to perform structure–function analyses (Fig. 7).

In contrast to mixed primary cerebellar cultures, where the yield of PNs is limited by the number of individual embryonic cerebella that can be processed, the differentiation of mESCs into PNs should be readily amendable to scale-up. This opens the possibility of performing high-throughput assays on PNs to identify small molecules that might serve as treatments for debilitating PN-related diseases. Our demonstration that GN precursors can be successfully cryopreserved should also

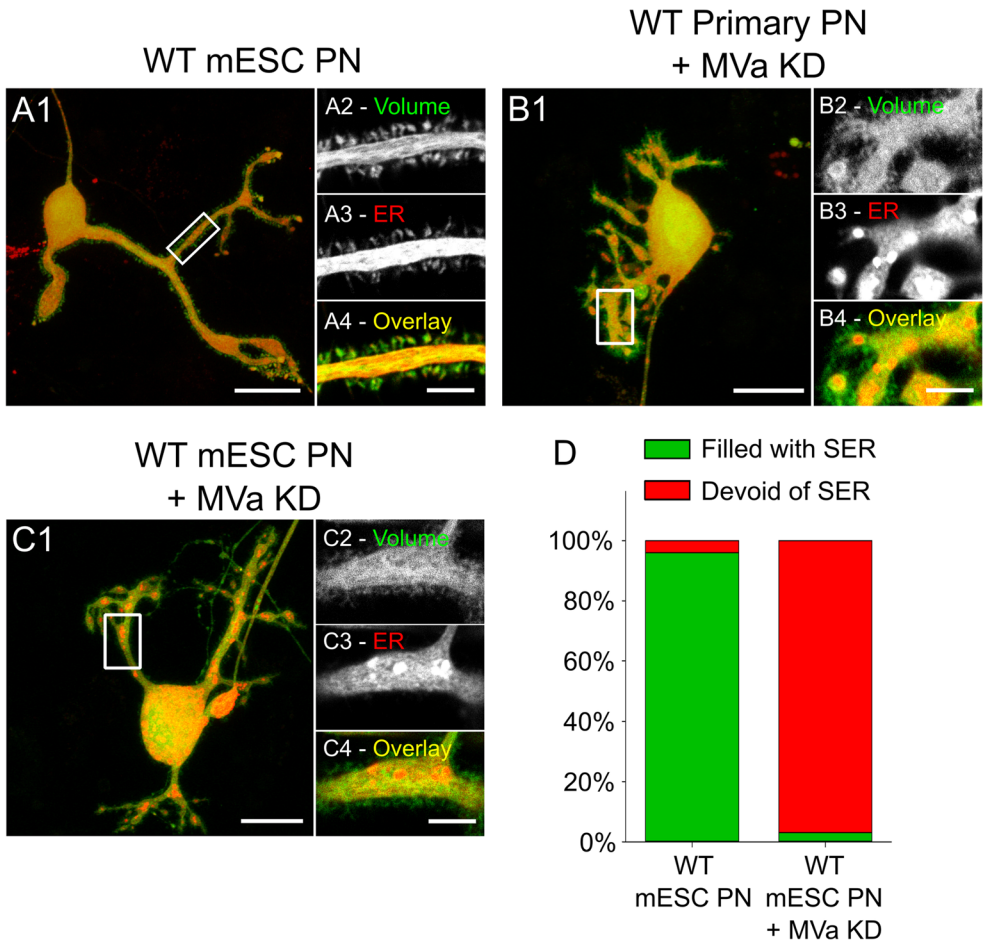

Fig. 7 miRNA-mediated knockdown of myosin Va in mESC-derived PNs phenocopies the defect in SER spine localization seen in primary PNs isolated from myosin Va-null mice. Shown are representative examples of an untreated WT mESC-derived PN present within a GN/PN co-culture (A1–A4), a WT primary PN expressing a validated miRNA against myosin Va (MVa KD) (B1–B4), and a WT mESC-derived PN present within a GN/PN co-culture expressing a validated miRNA against myosin Va (MVa KD) (C1–C4). All three cells were expressing GFP as a volume marker, and RFP-KDEL as an SER marker. Each sample is presented as a lower magnification, overlaid image in the first panel, and higher magnification split and overlaid images of the boxed region in the second, third, and fourth panels, respectively. Like WT primary PNs [10], most if not all the dendritic spines in WT mESC-derived PNs are filled with a tubule of SER (A1–A4). Like primary PNs isolated from *dilute lethal*/myosin Va-null PNs [10], most if not all the dendritic spines in WT primary PNs and WT mESC-derived PNs are devoid of SER following myosin Va knockdown (B1–B4 and C1–C4, respectively). Mag bars = 20 μm (A1–C1) and 5 μm (A4–C4). (D) Percent of spines filled with SER (green) or devoid of SER (red) for the indicated PNs. A total of six WT mESC-derived PNs and six myosin Va KD ESC-derived PNs from two independent preparations were scored for spine SER inheritance (n = 167 for WT mESC-derived PNs; n = 195 for KD mESC-derived PNs)

facilitate such screening efforts by allowing the stock piling of cells in advance.

Finally, the application of CRISPR/Cas9-based gene editing to mESCs prior to their differentiation into PNs should provide a powerful tool for studying the structure, function, and pathophysiology of PNs. For example, generating and characterizing PNs containing specific gene deletions by performing CRISPR/Cas9 on mESCs and then differentiating them into PNs will be much faster and less expensive than generating the corresponding mouse knockout to obtain primary mutant PNs. Moreover, gene-edited mESCs can be used to create mutant mice if one wishes to subsequently characterize phenotypes at the whole cerebellum/animal level [110, 111]. PNs derived from gene-edited mESCs will be particularly valuable when one must examine the function of a gene whose knockout in the mouse leads to early embryonic lethality. Indeed, the ability to edit genes in mESCs and then differentiate them into PNs opens up myriad possibilities for performing detailed structure–function studies of genes associated with SCAs and other diseases that affect PNs. Moreover, these gene-edited mESCs can then be used to generate mouse models for these diseases.

Acknowledgements We thank Dr. Chengyu Lui (NHLBI Transgenic Core) for providing the mouse embryonic stem cells.

Funding This study was funded by the National Heart, Lung, and Blood Institute Intramural Research Program at the National Institutes of Health.

Compliance with Ethical Standards

Conflict of Interest The authors declare that they have no conflict of interest.

Ethical Approval All animal care and experiments performed in this study were approved by the Institutional Animal Care and Use Committee of the National Heart, Lung, and Blood Institute in accordance with the National Institute of Health guidelines. This article does not contain any studies with human participants performed by any of the authors.

Publisher's Note Springer Nature remains neutral with regard to jurisdictional claims in published maps and institutional affiliations.

References

1. Marr D. A theory of cerebellar cortex. J Physiol. 1969;202:437–70. https://doi.org/10.1113/jphysiol.1969.sp008820.
2. Ito M. Cerebellar circuitry as a neuronal machine. Prog Neurobiol. 2006;78:272–303. https://doi.org/10.1016/J.PNEUROBIO.2006.02.006.
3. Heintz TG, Eva R, Fawcett JW. Regional regulation of Purkinje cell dendritic spines by integrins and Eph/ephrins. PLoS One. 2016;11:e0158558. https://doi.org/10.1371/journal.pone.0158558.
4. Bezprozvanny I. Calcium signaling and neurodegenerative diseases. Trends Mol Med. 2009;15:89–100. https://doi.org/10.1016/J.MOLMED.2009.01.001.
5. Paulson HL. The spinocerebellar ataxias. J Neuroophthalmol. 2009;29:227–37. https://doi.org/10.1097/WNO0b013e3181b416de.
6. Sun Y-M, Lu C, Wu Z-Y. Spinocerebellar ataxia: relationship between phenotype and genotype—a review. Clin Genet. 2016;90:305–14. https://doi.org/10.1111/cge.12808.
7. Orr HT, Chung M, Banfi S, Kwiatkowski TJ, Servadio A, Beaudet AL, et al. Expansion of an unstable trinucleotide CAG repeat in spinocerebellar ataxia type 1. Nat Genet. 1993;4:221–6. https://doi.org/10.1038/ng0793-221.
8. Trott A, Houenou LJ. Mini-review: spinocerebellar ataxias: an update of SCA genes. Recent Pat DNA Gene Seq. 2012;6:115–21.
9. Soong B-W, Morrison PJ. Spinocerebellar ataxias. Handb Clin Neurol. 2018:143–74. https://doi.org/10.1016/B978-0-444-64189-2.00010-X.
10. Wagner W, Brenowitz SD, Hammer JA. Myosin-Va transports the endoplasmic reticulum into the dendritic spines of Purkinje neurons. Nat Cell Biol. 2011;13:40–8. https://doi.org/10.1038/ncb2132.
11. Wagner W, McCroskery S, Hammer JA. An efficient method for the long-term and specific expression of exogenous cDNAs in cultured Purkinje neurons. J Neurosci Methods. 2011;200:95–105. https://doi.org/10.1016/j.jneumeth.2011.06.006.
12. Alexander CJ, Hammer JA. Optimization of cerebellar purkinje neuron cultures and development of a plasmid-based method for purkinje neuron-specific, miRNA-mediated protein knockdown. Methods Cell Biol. 2016;131:177–97. https://doi.org/10.1016/bs.mcb.2015.06.004.
13. Kim J-H, Auerbach JM, Rodríguez-Gómez JA, Velasco I, Gavin D, Lumelsky N, et al. Dopamine neurons derived from embryonic stem cells function in an animal model of Parkinson's disease. Nature. 2002;418:50–6. https://doi.org/10.1038/nature00900.
14. Wichterle H, Lieberam I, Porter JA, Jessell TM. Directed differentiation of embryonic stem cells into motor neurons. Cell. 2002;110:385–97. https://doi.org/10.1016/S0092-8674(02)00835-8.
15. Bain G, Kitchens D, Yao M, Huettner JE, Gottlieb DI. Embryonic stem cells express neuronal properties in vitro. Dev Biol. 1995;168:342–57. https://doi.org/10.1006/DBIO.1995.1085.
16. Zhang S-C, Wernig M, Duncan ID, Brüstle O, Thomson JA. In vitro differentiation of transplantable neural precursors from human embryonic stem cells. Nat Biotechnol. 2001;19:1129–33. https://doi.org/10.1038/nbt1201-1129.
17. Lee S-H, Lumelsky N, Studer L, Auerbach JM, McKay RD. Efficient generation of midbrain and hindbrain neurons from mouse embryonic stem cells. Nat Biotechnol. 2000;18:675–9. https://doi.org/10.1038/76536.
18. O'Shea KS. Embryonic stem cell models of development. Anat Rec. 1999;257:32–41. https://doi.org/10.1002/(SICI)1097-0185(19990215)257:1<32::AID-AR6>3.0.CO;2-2.
19. Sylvester KG, Longaker MT. Stem cells. Arch Surg. 2004;139:93–9. https://doi.org/10.1001/archsurg.139.1.93.
20. Temple S. The development of neural stem cells. Nat. 2001;4146859:2001.
21. Gage FH, Coates PW, Palmer TD, Kuhn HG, Fisher LJ, Suhonen JO, et al. Survival and differentiation of adult neuronal progenitor cells transplanted to the adult brain. Proc Natl Acad Sci. 1995;92:11879–83. https://doi.org/10.1073/pnas.92.25.11879.
22. Gage FH. Mammalian neural stem cells. Science. 2000;287(80):1433–8. https://doi.org/10.1126/science.287.5457.1433.
23. Reynolds B, Weiss S. Generation of neurons and astrocytes from isolated cells of the adult mammalian central nervous system. Science. 1992;255(80):1707–10. https://doi.org/10.1126/science.1553558.
24. Temple S. Stem cell plasticity—building the brain of our dreams. Nat Rev Neurosci. 2001;2:513–20. https://doi.org/10.1038/35081577.
25. Qian X, Shen Q, Goderie SK, He W, Capela A, Davis AA, et al. Timing of CNS cell generation. Neuron. 2000;28:69–80. https://doi.org/10.1016/S0896-6273(00)00086-6.
26. Li M, Pevny L, Lovell-Badge R, Smith A. Generation of purified neural precursors from embryonic stem cells by lineage selection. Curr Biol. 1998;8:971–S2. https://doi.org/10.1016/S0960-9822(98)70399-9.
27. Schuldiner M, Eiges R, Eden A, Yanuka O, Itskovitz-Eldor J, Goldstein RS, et al. Induced neuronal differentiation of human embryonic stem cells. Brain Res. 2001;913:201–5. https://doi.org/10.1016/S0006-8993(01)02776-7.
28. Itskovitz-Eldor J, Schuldiner M, Karsenti D, Eden A, Yanuka O, Amit M, et al. Differentiation of human embryonic stem cells into embryoid bodies compromising the three embryonic germ layers. Mol Med. 2000;6:88–95.
29. Desbaillets I, Ziegler U, Groscurth P, Gassmann M. Embryoid bodies: an in vitro model of mouse embryogenesis. Exp Physiol. 2000;85:645–51.
30. Tao O, Shimazaki T, Okada Y, Naka H, Kohda K, Yuzaki M, et al. Efficient generation of mature cerebellar Purkinje cells from mouse embryonic stem cells. J Neurosci Res. 2010;88:234–47. https://doi.org/10.1002/jnr.22208.
31. Muguruma K, Nishiyama A, Ono Y, Miyawaki H, Mizuhara E, Hori S, et al. Ontogeny-recapitulating generation and tissue integration of ES cell–derived Purkinje cells. Nat Neurosci. 2010;13:1171–80. https://doi.org/10.1038/nn.2638.
32. Wang S, Wang B, Pan N, Fu L, Wang C, Song G, et al. Differentiation of human induced pluripotent stem cells to mature functional Purkinje neurons. Sci Rep. 2015;5:9232. https://doi.org/10.1038/srep09232.
33. Brickman JM, Serup P. Properties of embryoid bodies. WIREs Dev Biol. 2017;6. https://doi.org/10.1002/wdev.259.

34. Su H-L, Muguruma K, Matsuo-Takasaki M, Kengaku M, Watanabe K, Sasai Y. Generation of cerebellar neuron precursors from embryonic stem cells. Dev Biol. 2006;290:287–96. https://doi.org/10.1016/J.YDBIO.2005.11.010.
35. Srivastava R, Kumar M, Peineau S, Csaba Z, Mani S, Gressens P, et al. Conditional induction of Math1 specifies embryonic stem cells to cerebellar granule neuron lineage and promotes differentiation into mature granule neurons. Stem Cells. 2013;31:652–65. https://doi.org/10.1002/stem.1295.
36. Lindholm D, Castrén E, Tsoulfas P, Kolbeck R, da Berzaghi MP, Leingärtner A, et al. Neurotrophin-3 induced by tri-iodothyronine in cerebellar granule cells promotes Purkinje cell differentiation. J Cell Biol. 1993;122:443–50. https://doi.org/10.1083/JCB.122.2.443.
37. Salero E, Hatten ME. Differentiation of ES cells into cerebellar neurons. Proc Natl Acad Sci. 2007;104:2997–3002. https://doi.org/10.1073/pnas.0610879104.
38. Crossley PH, Martinez S, Martin GR. Midbrain development induced by FGF8 in the chick embryo. Nature. 1996;380:66–8. https://doi.org/10.1038/380066a0.
39. Millen KJ, Steshina EY, Iskusnykh IY, Chizhikov VV. Transformation of the cerebellum into more ventral brainstem fates causes cerebellar agenesis in the absence of Ptf1a function. Proc Natl Acad Sci. 2014;111:E1777–86. https://doi.org/10.1073/pnas.1315024111.
40. Alder J, Cho NK, Hatten ME. Embryonic precursor cells from the rhombic lip are specified to a cerebellar granule neuron identity. Neuron. 1996;17:389–99. https://doi.org/10.1016/S0896-6273(00)80172-5.
41. Machold R, Fishell G. Math1 is expressed in temporally discrete pools of cerebellar rhombic-lip neural progenitors. Neuron. 2005;48:17–24. https://doi.org/10.1016/J.NEURON.2005.08.028.
42. Inman GJ, Nicolás FJ, Callahan JF, Harling JD, Gaster LM, Reith AD, et al. SB-431542 is a potent and specific inhibitor of transforming growth factor-beta superfamily type I activin receptor-like kinase (ALK) receptors ALK4, ALK5, and ALK7. Mol Pharmacol. 2002;62:65–74.
43. Ma X, Kawamoto S, Uribe J, Adelstein RS. Function of the neuron-specific alternatively spliced isoforms of nonmuscle myosin II-B during mouse brain development. Mol Biol Cell. 2006;17:2138–49. https://doi.org/10.1091/mbc.E05-10-0997.
44. Leitges M, Kovac J, Plomann M, Linden DJ. A unique PDZ ligand in PKCα confers induction of cerebellar long-term synaptic depression. Neuron. 2004;44:585–94. https://doi.org/10.1016/J.NEURON.2004.10.024.
45. Schindelin J, Arganda-Carreras I, Frise E, Kaynig V, Longair M, Pietzsch T, et al. Fiji: an open-source platform for biological-image analysis. Nat Methods. 2012;9:676–82. https://doi.org/10.1038/nmeth.2019.
46. Theodorou E, Dalembert G, Heffelfinger C, White E, Weissman S, Corcoran L, et al. A high throughput embryonic stem cell screen identifies Oct-2 as a bifunctional regulator of neuronal differentiation. Genes Dev. 2009;23:575–88. https://doi.org/10.1101/gad.1772509.
47. Katoh Y, Katoh M. Conserved POU-binding site linked to SP1-binding site within FZD5 promoter: transcriptional mechanisms of FZD5 in undifferentiated human ES cells, fetal liver/spleen, adult colon, pancreatic islet, and diffuse-type gastric cancer. Int J Oncol. 2007;30:751–5. https://doi.org/10.3892/ijo.30.3.751.
48. Zhang X, Huang CT, Chen J, Pankratz MT, Xi J, Li J, et al. Pax6 is a human neuroectoderm cell fate determinant. Cell Stem Cell. 2010;7:90–100. https://doi.org/10.1016/j.stem.2010.04.017.
49. Zhang J, Jiao J. Molecular biomarkers for embryonic and adult neural stem cell and neurogenesis. Biomed Res Int. 2015;2015:1–14. https://doi.org/10.1155/2015/727542.
50. Wen J, Hu Q, Li M, Wang S, Zhang L, Chen Y, et al. Pax6 directly modulate Sox2 expression in the neural progenitor cells. Neuroreport. 2008;19:413–17. https://doi.org/10.1097/WNR.0b013e3282f64377
51. Perrier AL, Tabar V, Barberi T, Rubio ME, Bruses J, Topf N, et al. Derivation of midbrain dopamine neurons from human embryonic stem cells. Proc Natl Acad Sci U S A. 2004;101:12543–8. https://doi.org/10.1073/pnas.0404700101.
52. Li X-J, Du Z-W, Zarnowska ED, Pankratz M, Hansen LO, Pearce RA, et al. Specification of motoneurons from human embryonic stem cells. Nat Biotechnol. 2005;23:215–21. https://doi.org/10.1038/nbt1063.
53. Chambers SM, Fasano CA, Papapetrou EP, Tomishima M, Sadelain M, Studer L. Highly efficient neural conversion of human ES and iPS cells by dual inhibition of SMAD signaling. Nat Biotechnol. 2009;27:275–80. https://doi.org/10.1038/nbt.1529.
54. Dou D, Zhao H, Li Z, Xu L, Xiong X, Wu X, et al. *CHD1L* promotes neuronal differentiation in human embryonic stem cells by upregulating *PAX6*. Stem Cells Dev. 2017;26:1626–36. https://doi.org/10.1089/scd.2017.0110.
55. Hu B-Y, Weick JP, Yu J, Ma L-X, Zhang X-Q, Thomson JA, et al. Neural differentiation of human induced pluripotent stem cells follows developmental principles but with variable potency. Proc Natl Acad Sci. 2010;107:4335–40. https://doi.org/10.1073/pnas.0910012107.
56. Ericson J, Rashbass P, Schedl A, Brenner-Morton S, Kawakami A, Van Heyningen V, et al. Pax6 controls progenitor cell identity and neuronal fate in response to graded Shh signaling. Cell. 1997;90:169–80. https://doi.org/10.1016/S0092-8674(00)80323-2.
57. Sansom SN, Griffiths DS, Faedo A, Kleinjan DJ, Ruan Y, Smith J, et al. The level of the transcription factor Pax6 is essential for controlling the balance between neural stem cell self-renewal and neurogenesis. PLoS Genet. 2009;5:e1000511. https://doi.org/10.1371/journal.pgen.1000511.
58. Don S, Verrills NM, Liaw TYE, Liu MLM, Norris MD, Haber M, et al. Neuronal-associated microtubule proteins class III beta-tubulin and MAP2c in neuroblastoma: role in resistance to microtubule-targeted drugs. Mol Cancer Ther. 2004;3:1137–46.
59. Morrison ME, Mason CA. Granule neuron regulation of Purkinje cell development: striking a balance between neurotrophin and glutamate signaling. J Neurosci. 1998;18:3563–73. https://doi.org/10.1523/JNEUROSCI.18-10-03563.1998.
60. Kuhar SG, Feng L, Vidan S, Ross ME, Hatten ME, Heintz N. Changing patterns of gene expression define four stages of cerebellar granule neuron differentiation. Neurobiology. 1993;117(1):97–104.
61. Nayler S, Vanichkina D, Kanjhan R, Taft R. Transcriptome of the developing ataxia-telangiectasia cerebellum: RNA sequencing of human iPSC-derived cerebellar progenitors. n.d. https://doi.org/10.13140/RG.2.1.5064.8400.
62. Ben-Arie N, Bellen HJ, Armstrong DL, McCall AE, Gordadze PR, Guo Q, et al. Math1 is essential for genesis of cerebellar granule neurons. Nature. 1997;390:169–72. https://doi.org/10.1038/36579.
63. Gazit R, Krizhanovsky V, Ben-Arie N, Samper E, Brown S, Aguilera RJ, et al. Math1 controls cerebellar granule cell differentiation by regulating multiple components of the Notch signaling pathway. Development. 2004;131:903–13. https://doi.org/10.1242/dev.00982.
64. Schüller U, Heine VM, Mao J, Kho AT, Dillon AK, Han Y-G, et al. Acquisition of granule neuron precursor identity is a critical determinant of progenitor cell competence to form Shh-induced medulloblastoma. Cancer Cell. 2008;14:123–34. https://doi.org/10.1016/J.CCR.2008.07.005.

65. Watson LM, Wong MMK, Vowles J, Cowley SA, Becker EBE. A simplified method for generating Purkinje cells from human-induced pluripotent stem cells. Cerebellum. 2018;17:419–27. https://doi.org/10.1007/s12311-017-0913-2.
66. Ryan KE, Kim PS, Fleming JT, Brignola E, Cheng FY, Litingtung Y, et al. Lkb1 regulates granule cell migration and cortical folding of the cerebellar cortex. Dev Biol. 2017;432:165–77. https://doi.org/10.1016/J.YDBIO.2017.09.036.
67. Wefers AK, Lindner S, Schulte JH, Schüller U. Overexpression of Lin28b in neural stem cells is insufficient for brain tumor formation, but induces pathological lobulation of the developing cerebellum. Cerebellum. 2017;16:122–31. https://doi.org/10.1007/s12311-016-0774-0.
68. McDougall ARA, Hale N, Rees S, Harding R, De Matteo R, Hooper SB, et al. Erythropoietin protects against lipopolysaccharide-induced microgliosis and abnormal granule cell development in the ovine fetal cerebellum. Front Cell Neurosci. 2017;11:224. https://doi.org/10.3389/fncel.2017.00224.
69. Wechsler-Reya RJ, Scott MP. Control of neuronal precursor proliferation in the cerebellum by sonic hedgehog. Neuron. 1999;22:103–14. https://doi.org/10.1016/S0896-6273(00)80682-0.
70. Falsig J, Sonati T, Herrmann US, Saban D, Li B, Arroyo K, et al. Prion pathogenesis is faithfully reproduced in cerebellar organotypic slice cultures. PLoS Pathog. 2012;8:e1002985. https://doi.org/10.1371/journal.ppat.1002985.
71. Levin SI, Khaliq ZM, Aman TK, Grieco TM, Kearney JA, Raman IM, et al. Impaired motor function in mice with cell-specific knockout of sodium channel *Scn8a* (Na_V 1.6) in cerebellar Purkinje neurons and granule cells. J Neurophysiol. 2006;96:785–93. https://doi.org/10.1152/jn.01193.2005.
72. Martenson JS, Yamasaki T, Chaudhury NH, Albrecht D, Tomita S. Assembly rules for GABAA receptor complexes in the brain. Elife. 2017;6. https://doi.org/10.7554/eLife.27443.
73. Aller MI, Jones A, Merlo D, Paterlini M, Meyer AH, Amtmann U, et al. Cerebellar granule cell Cre recombinase expression. Genesis. 2003;36:97–103. https://doi.org/10.1002/gene.10204.
74. Wang B, Harrison W, Overbeek PA, Zheng H. Transposon mutagenesis with coat color genotyping identifies an essential role for Skor2 in sonic hedgehog signaling and cerebellum development. Development. 2011;138:4487–97. https://doi.org/10.1242/dev.067264.
75. Nakatani T, Minaki Y, Kumai M, Nitta C, Ono Y. The c-Ski family member and transcriptional regulator Corl2/Skor2 promotes early differentiation of cerebellar Purkinje cells. Dev Biol. 2014;388:68–80. https://doi.org/10.1016/J.YDBIO.2014.01.016.
76. Skinner PJ, Vierra-Green CA, Clark HB, Zoghbi HY, Orr HT. Altered trafficking of membrane proteins in Purkinje cells of SCA1 transgenic mice. Am J Pathol. 2001;159:905–13. https://doi.org/10.1016/S0002-9440(10)61766-X.
77. Laure-Kamionowska M, Maślińska D. Calbindin positive Purkinje cells in the pathology of human cerebellum occurring at the time of its development. Folia Neuropathol. 2009;47:300–5.
78. Liu Y, Lee JW, Ackerman SL. Mutations in the microtubule-associated protein 1A (Map1a) gene cause Purkinje cell degeneration. J Neurosci. 2015;35:4587–98. https://doi.org/10.1523/JNEUROSCI.2757-14.2015.
79. Sillitoe RV, Stephen D, Lao Z, Joyner AL. Engrailed homeobox genes determine the organization of Purkinje cell sagittal stripe gene expression in the adult cerebellum. J Neurosci. 2008;28:12150–62. https://doi.org/10.1523/JNEUROSCI.2059-08.2008.
80. Sarna JR, Marzban H, Watanabe M, Hawkes R. Complementary stripes of phospholipase Cβ3 and Cβ4 expression by Purkinje cell subsets in the mouse cerebellum. J Comp Neurol. 2006;496:303–13. https://doi.org/10.1002/cne.20912.
81. Oue M, Handa H, Matsuzaki Y, Suzue K, Murakami H, Hirai H. The murine stem cell virus promoter drives correlated transgene expression in the leukocytes and cerebellar Purkinje cells of transgenic mice. PLoS One. 2012;7:e51015. https://doi.org/10.1371/journal.pone.0051015.
82. Miller TE, Wang J, Sukhdeo K, Horbinski C, Tesar PJ, Wechsler-Reya RJ, et al. Lgr5 marks post-mitotic, lineage restricted cerebellar granule neurons during postnatal development. PLoS One. 2014;61:288. https://doi.org/10.3311/PPch.10689.
83. Zhang J, D'Ercole AJ. Expression of Mcl-1 in cerebellar granule neurons is regulated by IGF-I in a developmentally specific fashion. Dev Brain Res. 2004;152:255–63. https://doi.org/10.1016/j.devbrainres.2004.07.008.
84. O'Hearn E, Molliver ME. Degeneration of Purkinje cells in parasagittal zones of the cerebellar vermis after treatment with ibogaine or harmaline. Neuroscience. 1993;55:303–10. https://doi.org/10.1016/0306-4522(93)90500-F.
85. Luo L, Hensch TK, Ackerman L, Barbel S, Jan LY, Jan YN. Differential effects of the Rac GTPase on Purkinje cell axons and dendritic trunks and spines. Nature. 1996;379:837–40. https://doi.org/10.1038/379837a0.
86. Yang Q, Hashizume Y, Yoshida M, Wang Y, Goto Y, Mitsuma N, et al. Morphological Purkinje cell changes in spinocerebellar ataxia type 6. Acta Neuropathol. 2000;100:371–6. https://doi.org/10.1007/s004010000201.
87. Alexander CJ, Wagner W, Copeland NG, Jenkins NA, Hammer JA. Creation of a myosin Va-TAP tagged mouse and identification of potential myosin Va-interacting proteins in the cerebellum. Cytoskeleton. 2018;75:395–409. https://doi.org/10.1002/cm.21474.
88. McGee AW, Topinka JR, Hashimoto K, Petralia RS, Kakizawa S, Kauer F, et al. PSD-93 knock-out mice reveal that neuronal MAGUKs are not required for development or function of parallel fiber synapses in cerebellum. J Neurosci. 2001;21:3085–91.
89. Miyazaki T, Watanabe M, Yamagishi A, Takahashi M. B2 exon splicing of nonmuscle myosin heavy chain IIB is differently regulated in developing and adult rat brain. Neurosci Res. 2000;37:299–306. https://doi.org/10.1016/S0168-0102(00)00130-9.
90. Miyata M, Miyata H, Mikoshiba K, Ohama E. Development of Purkinje cells in humans: an immunohistochemical study using a monoclonal antibody against the inositol 1,4,5-triphosphate type 1 receptor (IP3R1). Acta Neuropathol. 1999;98:226–32.
91. Hisatsune C, Miyamoto H, Hirono M, Yamaguchi N, Sugawara T, Ogawa N, et al. IP3R1 deficiency in the cerebellum/brainstem causes basal ganglia-independent dystonia by triggering tonic Purkinje cell firings in mice. Front Neural Circuits. 2013;7:156. https://doi.org/10.3389/fncir.2013.00156.
92. Kawaai K, Mizutani A, Shoji H, Ogawa N, Ebisui E, Kuroda Y, et al. IRBIT regulates CaMKIIα activity and contributes to catecholamine homeostasis through tyrosine hydroxylase phosphorylation. Proc Natl Acad Sci U S A. 2015;112:5515–20. https://doi.org/10.1073/pnas.1503310112.
93. Yang D, Shcheynikov N, Muallem S. IRBIT: it is everywhere. Neurochem Res. 2011;36:1166–74. https://doi.org/10.1007/s11064-010-0353-6.
94. Takagishi Y, Oda S, Hayasaka S, Dekker-Ohno K, Shikata T, Inouye M, et al. The dilute-lethal (dl) gene attacks a Ca2+ store in the dendritic spine of Purkinje cells in mice. Neurosci Lett. 1996;215:169–72. https://doi.org/10.1016/0304-3940(96)12967-0.
95. Dekker-Ohno K, Hayasaka S, Takagishi Y, Oda S, Wakasugi N, Mikoshiba K, et al. Endoplasmic reticulum is missing in dendritic spines of Purkinje cells of the ataxic mutant rat. Brain Res. 1996;714:226–30.
96. Richter K, Langnaese K, Kreutz MR, Olias G, Zhai R, Scheich H, et al. Presynaptic cytomatrix protein Bassoon is localized at both

excitatory and inhibitory synapses of rat brain. J Comp Neurol. 1999;408:437–48. https://doi.org/10.1002/(SICI)1096-9861(19990607)408:3<437::AID-CNE9>3.0.CO;2-5.
97. Wang W, Stock RE, Gronostajski RM, Wong YW, Schachner M, Kilpatrick DL. A role for nuclear factor I in the intrinsic control of cerebellar granule neuron gene expression. J Biol Chem. 2004;279:53491–7. https://doi.org/10.1074/jbc.M410370200.
98. Yuzaki M, Forrest D, Verselis LM, Sun SC, Curran T, Connor JA. Functional NMDA receptors are transiently active and support the survival of Purkinje cells in culture. J Neurosci. 1996;16:4651–61. https://doi.org/10.1523/JNEUROSCI.16-15-04651.1996.
99. Linden DJ, Connor JA. Participation of postsynaptic PKC in cerebellar long-term depression in culture. Science. 1991;254:1656–9.
100. Ahn S, Ginty DD, Linden DJ. A late phase of cerebellar long-term depression requires activation of CaMKIV and CREB. Neuron. 1999;23:559–68. https://doi.org/10.1016/S0896-6273(00)80808-9.
101. Südhof TC. The presynaptic active zone. Neuron. 2012;75:11–25. https://doi.org/10.1016/J.NEURON.2012.06.012.
102. Dieck S, Sanmartí-Vila L, Langnaese K, Richter K, Kindler S, Soyke A, et al. Bassoon, a novel zinc-finger CAG/glutamine-repeat protein selectively localized at the active zone of presynaptic nerve terminals. J Cell Biol. 1998;142:499–509. https://doi.org/10.1083/JCB.142.2.499.
103. Nomura T, Kakegawa W, Matsuda S, Kohda K, Nishiyama J, Takahashi T, et al. Cerebellar long-term depression requires dephosphorylation of TARP in Purkinje cells. Eur J Neurosci. 2012;35:402–10. https://doi.org/10.1111/j.1460-9568.2011.07963.x.
104. Seki T, Yoshino K, Tanaka S, Dohi E, Onji T, Yamamoto K, et al. Establishment of a novel fluorescence-based method to evaluate chaperone-mediated autophagy in a single neuron. PLoS One. 2012;7:e31232. https://doi.org/10.1371/journal.pone.0031232.
105. Shimobayashi E, Kapfhammer JP. Increased biological activity of protein kinase C gamma is not required in spinocerebellar ataxia 14. Mol Brain. 2017;10:34. https://doi.org/10.1186/s13041-017-0313-z.
106. Miyata M, Finch EA, Khiroug L, Hashimoto K, Hayasaka S, Oda S-I, et al. Local calcium release in dendritic spines required for long-term synaptic depression. Neuron. 2000;28:233–44. https://doi.org/10.1016/S0896-6273(00)00099-4.
107. Takagishi Y, Hashimoto K, Kayahara T, Watanabe M, Otsuka H, Mizoguchi A, et al. Diminished climbing fiber innervation of Purkinje cells in the cerebellum of myosin Va mutant mice and rats. Dev Neurobiol. 2007;67:909–23. https://doi.org/10.1002/dneu.20375.
108. Takagishi Y, Murata Y. Myosin Va mutation in rats is an animal model for the human hereditary neurological disease, Griscelli syndrome type 1. Ann N Y Acad Sci. 2006;1086:66–80. https://doi.org/10.1196/annals.1377.006.
109. Kim Y, Kim T, Rhee JK, Lee D, Tanaka-Yamamoto K, Yamamoto Y. Selective transgene expression in cerebellar Purkinje cells and granule cells using adeno-associated viruses together with specific promoters. Brain Res. 1620;2015:1–16. https://doi.org/10.1016/j.brainres.2015.05.015.
110. Hall B, Limaye A, Kulkarni AB. Overview: generation of gene knockout mice. Curr Protoc Cell Biol 2009;Chapter 19:Unit 19.12 19.12.1–17. https://doi.org/10.1002/0471143030.cb1912s44.
111. Longenecker G, Kulkarni AB. Generation of gene knockout mice by ES cell microinjection. Curr Protoc Cell Biol 2009;Chapter 19: Unit 19.14 19.14.1–36. https://doi.org/10.1002/0471143030.cb1914s44.